Spin triplet supercurrents in thin films of ferromagnetic CrO2

Anwar, M.S.

Chapter 6

Anisotropic magnetothermoelectric power of ferromagnetic thin films

We discuss measurements of the magnetothermoelectric power (MTEP) in metallic ferromagnetic films of $Ni_{80}Fe_{20}$ (Permalloy; Py), Co and CrO_2 at temperatures in the range of 100 K to 400 K. In Py and Co both the anisotropic magnetoresistance (AMR) and MTEP show a relative change in resistance and thermopower of the order of 0.2% when the magnetic field is reversed, and in both cases there is no significant change in AMR or MTEP after the saturation field has been reached. The data on CrO_2 show a different picture. Films were grown on TiO_2 and on sapphire. The MTEP behavior at low fields shows peaks similar to the AMR in these films, with variations up to 1%. With increasing field both the MR and the MTEP variations keeps growing, with MTEP showing relative changes of 1.5% with the thermal gradient along the *b*-axis and even 20% with the gradient along the *c*-axis, with an intermediate value of 3% for the film on sapphire. It appears that the low-field effects are due to the magnetic domain state, and the high-field effects are intrinsic to the electronic structure of CrO_2.

6.1 Introduction

Thermoelectric effects are the interplay between charge and heat currents. Among these are the Seebeck Effect (initially discovered by Seebeck in the 1820s [71]), the induction of an electrostatic potential across a conductor when it is exposed to temperature gradient ΔT; and the reverse phenomenon i.e. the emergence of ΔT on applying a potential difference across the conductor (the Peltier effect). When a conductor is subjected to a magnetic field B perpendicular to ΔT an electric field is induced normal to B and ΔT, which is called the Nernst Effect; its reverse is the Ettingshausen effect. Earlier work on field dependent thermoelectric power (TEP) in magnetic materials was done to investigate the phonon drag and magnon drag contribution in TEP along with diffusive thermopower.

Heat transport in a conductor is directly related to its electronic transport, in particular to charge transport. The discovery of *Giant Magnetoresistance* (GMR) [66] added another degree of freedom of spin to transport properties, that of spin. Thermal transport was investigated in ferromagnet/normal metal (F/N) multilayer (Fe/Cr, Fe/Co, Co/Cu), and large magneto-thermoelectric power (MTEP) effects were found upon applying a magnetic field [67–70]. They are similar to GMR and derive from similar mechanisms such as spin dependent scattering and spin accumulation at interfaces. The spin dependent scattering generates the spin dependent Seebeck coefficients.

For a ferromagnetic metal, spin currents can therefore be of separate importance and the new field of *Spin Caloritronics* is emerging to study heat transport by the spin system [65]. The idea of spin dependent Seebeck coefficients stimulated the discovery of the so-called *Spin Seebeck effect* (SSE) where a spin current is generated in a ferromagnetic layer under the influence of temperature gradient [71]. For these studies, thin films of $Ni_{80}Fe_{20}$ (Permallay, Py) were used, which have a modest spin polarization of 45%, but where magnetic domain switching can be effected at low applied fields.

Both magnetic-TEP (MTEP), and SSE are therefore of increasing fundamental interest. MTEP was recently investigated in the ferromagnetic semiconductor (Ga,Mn)As and was found related to the anisotropic magnetoresistance (AMR), and the Planar Hall effect (PHE) [72]. An Anomalous Nernst effect (ANE) was also observed when applied field was perpendicular to the sample plane, in relation with Anomalous Hall effect (AHE) [73].

Still, MTEP studies on ferromagnetic metals are few. Here we study MTEP in thin films of CrO_2 (fully spin polarized), and compare it to MTEP in films of partially spin polarized Co, Py and a bilayer CuNi/Py. We find that MTEP is closely related to the AMR and/or MR effects. But MTEP signal is significantly larger than MR signal for all ferromagnetic samples. Surprisingly,

we observed an opposite sign for MTEP in Co and Py thin films. Co shows negative MTEP while Py shows the positive effect.

This chapter contains the following sections. The theoretical concepts of thermal transport are discussed in Section 1.2. The fabrication of a thermal transport sample holder is described in Section 1.3. The results from different samples are given in Section 1.4. They are discussed in Section 1.5 and Section 1.6 gives a conclusion.

6.2 Thermal transport phenomena

Heat transport can be treated in the same fashion as charge transport. In semiclassical theory, the starting point is a collection of electrons in a crystal. The electrons are characterised by their wave vector and the occupation of different k-states is controlled by (i) the crystal band structure (ii) their wave-vector dependent energy $\epsilon(k)$.

At finite temperature and in equilibrium, the distribution over k-states is given by the Fermi-Dirac function,

$$\mathbf{f_k^o} = \frac{1}{e^{\frac{\epsilon(k)-\mu}{k_B T}} + 1} \tag{6.1}$$

where μ is the electrochemical potential. Generally, a charge current is given by the expression [74, 75],

$$\mathbf{J} = \frac{e}{4\pi^3} \int_{-\infty}^{+\infty} \upsilon_k f_k(r) d^3k \tag{6.2}$$

where υ_k is the electron band velocity and $f_k(r)$ a local distribution function. In equilibrium $f_k(r) = f_k^o$ and $\mathbf{J} = 0$, because positive and negative $k-$states are equally occupied. Currents (charge or heat) start to flow when spatially varying electric fields, magnetic fields, or temperatures are applied. Transport then can be expressed in terms of a function $g_k(r)$ which expresses the deviation from equilibrium.

$$g_k(r) = f_k(r) - f_k^o \tag{6.3}$$

A transport equation called the Boltzmann equation, can now be set-up by considering processes which change the local distribution function $f_k(r)$. In its simplest form, the processes to consider are (i) diffusion of the carrier, and

(ii) charges induced by an electric field $\mathbf{E}$ or a magnetic field H, (iii) elastic scattering by impurities, lattice imperfections etc.

For the case of temperature gradients in particular, an additioanl assumption has to be made, namely that the local temperature $T(r)$ is well defined. Spatial derivatives of distribution functions such as g_k or f_k^o then also involve the temperature gradient ΔT.

The standard way to obtain an equation for $g_k(r)$ is to introduce the so-called relaxation-time apparoximation in order to deal with the scattering term. It assumes there is a relaxation time τ which is independent of energy or position, which brings the out-of-equilibrium functions to 0 when fields or gradients are turned off,

$$\frac{\partial g_k}{\partial t} = \frac{g_k}{\tau} \tag{6.4}$$

The final form of the g_k then reads,

$$g_k(r) = -\frac{\partial f_k^o}{\partial \epsilon}\tau v_k. \left\{ \frac{\epsilon(k)-\mu}{T}(-\nabla T) + e\left(E - \frac{1}{e}\nabla\mu\right)\right\} \tag{6.5}$$

The charge current follows from combining Eq. 6.2 and Eq. 6.5. The heat current w is defined through,

$$w = 2\int f_k \left\{\epsilon(k)-\mu\right\} v_k dk \tag{6.6}$$

It follows that for $\mathbf{J}$ and w can be written,

$$J = e^2 K_o.E + \frac{e}{T}K_1.(-\nabla T) \tag{6.7}$$

$$w = eK_1.E + \frac{1}{T}K_2.(-\nabla T) \tag{6.8}$$

where K_n are integrals involving Fermi functions and velocities. In terms of these equations, the electrical conductivity σ is given by $\sigma = e^2 K_o$, and the thermal conductivity κ by $\kappa = \frac{1}{T}K_2$. In an open circit condition ($\mathbf{J} = 0$). Eq. 6.8 can be written as,

$$E = \frac{1}{eT}K_o^{-1}K_1.(-\nabla T) = S(-\nabla T) \tag{6.9}$$

Here, S is the thermoelectric power (TEP) coefficient also known as the Seebeck coefficient, and the quantity to be measured in experiment . Similarly, the case of $\Delta T = 0$ can be considered. Eqs. 6.7 and 6.8 show there will still be heat transport,

$$w = eK_1.E = \frac{1}{e}K_o^{-1}K_1 J = \frac{eK_1}{\sigma}J = \Pi J \tag{6.10}$$

Here, Π is the Peltier coefficient, related to the Seebeck coefficient by $\Pi = ST$.

Mott and Jones derive a further expression for S by expanding the integrands for K_o and K_1. It can be found that [76],

$$K_1 = \frac{1}{3}\pi^2(k_B T)^2 \left[\frac{\partial}{\partial\epsilon}K_o(\epsilon)\right]_{\epsilon=\mu} \tag{6.11}$$

so that

$$S = \frac{\pi^2}{3}\frac{k_B^2}{e}\frac{T}{K_o}\left[\frac{\partial}{\partial\epsilon}K_o(\epsilon)\right]_{\epsilon=\mu} \tag{6.12}$$

$$S = \frac{\pi^2}{3}\frac{k_B^2}{e}T\left[\frac{\partial}{\partial\epsilon}ln\sigma(\epsilon)\right]_{\epsilon=\mu} \tag{6.13}$$

$$S = -eL_o T\partial_\epsilon ln\sigma(\epsilon)_{\epsilon_F} \tag{6.14}$$

Here, L_o is the Lorentz number, which is a universal quantity $L_0 = 2.45 \times 10^{-8} W\Omega K^{-2}$. Since the electrical conductivity in metals is directly proportional to the DOS at the Fermi energy $N(\epsilon_F)$, with energy-dependent mean free path λ_ϵ and relaxation time τ_ϵ,

$$\sigma_\epsilon = \frac{e^2\lambda_\epsilon^2}{\tau_\epsilon}.N(\epsilon) \tag{6.15}$$

Therefore,

$$\partial ln\sigma_{\epsilon_F} = \frac{N'(\epsilon_F)}{N(\epsilon_F)} + \frac{\lambda'}{\lambda} - \frac{\tau'}{\tau} \tag{6.16}$$

If the variations of the mean free path and of the scattering rates compared to the variation of the DOS, we obtain the formula,

$$S = -eL_oT\frac{N'(\epsilon_F)}{N(\epsilon_F)} \tag{6.17}$$

which is known as Mott's Law of TEP [77]. The important point here is that the Seebeck coefficient depends on the derivative of the DOS and in that sense is different from a quantity such as the specific heat, which depends on the DOS itself.

Mott's expression also illustrates the direct relation of thermopower with temperature. TEP is linear with T which is true for only diffusive contribution to the TEP. A T^3 dependence arises if the phonon drag phenomenon is also contributing and we write the relation for TEP as,

$$S = AT + BT^3 \tag{6.18}$$

In most of the noble metals, particularly monovalent ones, a peak in the temperature dependent TEP is observed at around 60 K. Such a departure from the linear relation is initiated by phonon drag. In polyvalent metals an anisotropic effect is also observed with a different response of TEP for different crystallographic orientations. Especially in Cd and Zr the TEP has different signs when ΔT is applied parallel and perpendicular to the hexagonal crystal axis at temperatures lower than 150 K [78]. This is expected for anisotropic phonon-phonon, phonon-electron and phonon-imperfection scatterings.

In a ferromagnetic material the magnon drag phenomenon can also contribute along with diffusive and phonon drag TEP. The magnon drag part is dependent on $T^{3/2}$ which makes it difficult to differentiate the both phonon and magnon contributions [75].

Equation 6.17 is valid for a conductor having only one kind of carriers. If a material has different kinds of carriers with different DOS at the Fermi level, such as a ferromagnet or a semiconductor they contribute separately. For a ferromagnet a two-spin current model can be used to calculate the total TEP and Mott's Law can be written as [78],

$$S = -eL_oT\left\{\frac{N'_\uparrow(\epsilon_F)}{N(\epsilon_F)} + \frac{N'_\downarrow(\epsilon_F)}{N(\epsilon_F)}\right\} = (S_\uparrow + S_\downarrow) \tag{6.19}$$

where $N(\epsilon_F) = N_\uparrow(\epsilon_F) + N_\downarrow(\epsilon_F)$, $S_{\uparrow(\downarrow)}$ is the Seebeck coefficient for spin up (spin down) electrons.

As noted, this is valid in situations when λ_ϵ and τ_ϵ do not vary signigicantly. In inhomogeneous systems such as magnetic multilayer, or magnets in a domain state, this will be different. For instance, Piraux *et al.* [79] investigated the consequences of electron-magnon scattering in the framework of GMR, which is instructive to mention here. A spin down (up) electron of wave vector k can be scattered into a spin up (down) state with wave vector $k' = k \pm q$ create (annihilation) of a magnon with wave vector q. The magnon energy E_q will transfer to or from the electron. This rise to a maximum scattering rate for spin up electrons with energies below the Fermi level ϵ_F, and/or spin down electrons with energies above. As a result the relaxation rate at ϵ_F will have different signs and opposite effect for a spin down electron. That gave rise to maximum rate of scattering below and above the Fermi level for spin up and spin down electron respectively. As a result, the magnon scattering contribution to the thermopower S^m is given by,

$$S^m_{\uparrow(\downarrow)} = \mp \frac{L_o}{k_B} \tag{6.20}$$

So,

$$S^m = \frac{N_\uparrow(\epsilon_F) S^m_\uparrow + N_\downarrow(\epsilon_F) S^m_\downarrow}{N_\downarrow(\epsilon_F) + N_\downarrow(\epsilon_F)} \tag{6.21}$$

Note, this contribution to the thermopower will go to zero for weak ferromagnets where the difference between the DOS for spin-up and spin-down is small. Otherwise, the difference for the different spin channels has consequences for the TEP in F/N multilayers when the magnetic configuration is changed from parallel to antiparalle.

6.3 Experimental

The Seebeck coefficient was measured using a home-made sample holder built on a PPMS puck. It consists of two copper blocks separated by a thermal insulator plastic. The copper has a high thermal conductance so the blocks are at a uniform temperature while a temperature gradient is produced between them. A small heater (maximum power of 5 W) is installed in the upper block. Its temperature is measured with a Pt-100 resistor and controlled with an external temperature controller. The temperature of the lower block is controlled by the set point of the PPMS, but the temperature was separately measured by a second Pt-100 resistor. The whole setup is covered with a

stainless steal cup that isolates the sample holder to help stabilize the temperature gradient. The measurements were done in a relatively low vacuum of 10 mTorr. A schematic of the sample holder is given in Fig.6.1

The samples consisted of thin films, mostly on sapphire substrates, with an area of 10×10 mm^2. CrO_2 films were deposited by Chemical Vapor Deposition (CVD) on both isostructural $TiO_2(100)$ and sapphire (1000) substrates. CrO_2 films deposit epitaxially on TiO_2 in the form of rectangular grains aligned along *c*-axis but on sapphire the grains are aligned with six fold rotational symmetry coming from the hexagonal structure of the substrate, as detailed in Chapter 3. The Py thin films were deposited using dc sputtering in a UHV sputtering system, with a base pressure of 10^{-9} mbar, the Co films were deposited in Z-400 an RF sputtering system with base pressure of 10^{-6} mbar. Both Py and Co were deposited on sapphire substrates because of its better thermal conductivity.

The Seebeck coefficient was recorded with reference to copper since Cu wires were connected at both ends of the film via pressed Indium. The potential difference was probed using a Nanovoltmeter (Keithley 2018) in an open circuit geometry ($J = 0$). A dynamic technique was utilized to measure TEM as function of temperature in which the temperature difference between hot and cold point was always 5 K, while the temperature of the cold point was increased by 10 K in each step. In this way hot point and cold point interchanged in each step between the temperature range of 100 - 400 K [80].

To check the setup, TEP was measured for nonmagnetic Cu, Au, and Pt with reference to Cu. In principal, it should give a zero TEP on a Cu thin film, but we measured around 2.5 μV at temperature difference of 45 K with the hot terminal being at 300 K, which gives a TEP of the order of 0.05 μV/K. The small TEP measured with the Cu film validates the assumption that we can take Cu as a reference for the TEP measurements and it also the test of our home-built sample holder. The non-zero voltage appearing on Cu thin films can be attributed to two factors. Firstly, we used pressed Indium to contact the Cu wires with samples that can also contribute to the TEP. Secondly, the Cu wires may not be connected really with the temperature bath, which can still generate some temperature difference between the voltage pads.

TEP measurements on Au and Pt unstructured thin films (100 nm and 10 nm thick, respectively) gave values of -0.4 μV/K and -5.8 μV/K reference to Cu. From the definition in Eq. 7.9 this means the voltage difference between the hot and the cold point is positive.

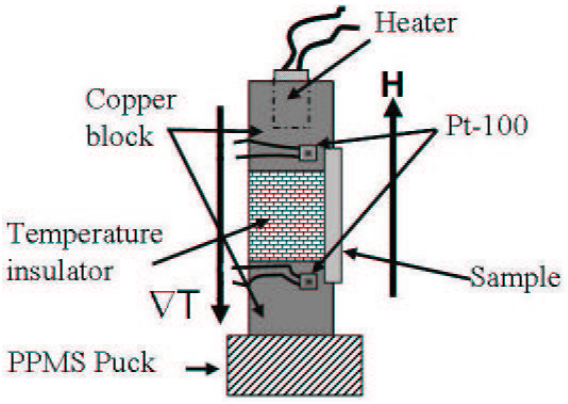

Figure 6.1: A schematic of thermal transport sample holder built on a PPMS puck. Two copper blocks separated by a thermally insulator plastic, a heater is installed in the upper Cu block and two Pt-100 resistor are being used to measure the temperature difference between the Cu blocks. Whole set up is covered with a stainless steel cap that is not shown in this picture.

6.4 Results

TEP was measured on unstructured thin films (10×10 mm^2) of Fe(25), Co(50), Py(25) and CrO_2(100) (the numbers in the parenthesis are the thicknesses) and the values are given in Fig. 6.2 in comparison with literature values taken form the Refs. [71, 81–86]. The absolute TEP of Au at 300 K is 1.94 μV/K, whereas for Cu, it is 1.84 μV/K, which makes TEP of Au in reference to Cu to be +0.1 μV/K. We measured a coefficient of -0.4 μV/K at room temperature. The sign change indicates a role of the In, since the absolute TEP of In is around 1.5 μV/K at room temperature [87], giving a negative TEP in reference to Cu bigger than Au.

Other reasons for these differences can be the effect of an oxide layer on the films and the thickness of the films. For instance, for thin films of Fe the value can be very different from bulk [85], comparable to the value of 2 μV/K as we measured. To completely answer this question we would need to measure the TEP of several films with different thicknesses, which we did not do because the homogeneity of the temperature gradient is a more important question than getting a very precise value for the absolute TEP of the films.

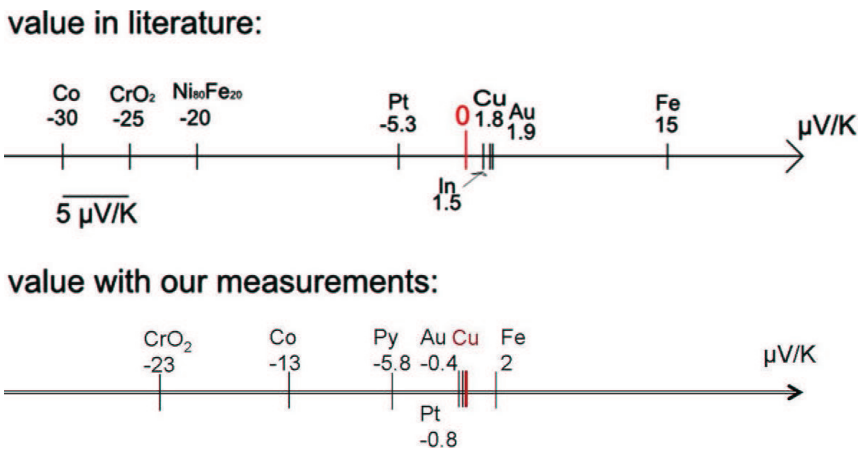

Figure 6.2: A comparison of our measurements of TEP (Seebeck coefficient) at room temperature for various materials with literature values. At the top the absolute values are given. At bottom, in our measurements Cu is being used as a reference metal, so all the values are given reference to with Cu. The CrO_2 thin films have anisotropic TEP, the given value is measured when ΔT was applied along the *b*-axis; TEP along the *c*-axis is about -3 μV/K.

6.4.1 Py and Co

Figure 6.3a shows the temperature dependent TEP of a 25 nm thick Py film deposited on a sapphire substrate. It shows roughly linear behavior with TEP = -7.8 μV/K at 300 K. It is a smaller value than the value reported in the literature, -20 μV/K [71] or -15 μV/K, [86]. The reasons for these differences can be the effect of oxide layer on these films and/or dimensionality of the samples in the form of thin films [85].

Next, a magnetic field $H||\Delta T$ is applied and TEP measured. We use the absolute values of the TEP to define the magnetic TEP, as follows:

$$MTEP = \frac{|TEP(H)| - |TEP_{max/min}|}{|TEP_{max/min}|} \tag{6.22}$$

where TEP_{max} or TEP_{min} are the maximum or minimum values of TEP at same low field (mostly, at coercive fields, peaks values). As a consequence, a positive relative change means an increase in TEP with field and vice versa. Figure 6.3b is presenting TEP as a function of externally applied field in parallel configuration (ΔT || H) on Py at an average temperature $\bar{T}$ = 178 K

and $\Delta T = 45$ K. It is obvious that sharp peaks appear at 0.2 mT and -0.2 mT corresponding to the coercive fields. The TEP is higher in the saturation state and lower in a domain state with a relative change of 0.2%. Such a behavior of MTEP is similar to the positive AMR effect (lower resistance in domain state) in Py films, as elaborated in Fig. 6.3c. The same effect is observed for a 50 nm thick Co thin film (see Fig. 6.3d), where peaks are appearing at -0.7 mT and 3.8 mT. It is interesting to note that for Co the TEP is *lower* in saturation state and *higher* in the domain state, opposite to the films of Py, although both Co and Py have the same sign of TEP and AMR. The MTEP for both films saturates just as magnetization or AMR. The hysteretic behaviour of MTEP and peaks around the coercive field reveal the direct connection of MTEP with the magnetization orientation in the films so we termed it anisotropic-MTEP (AMTEP). For both films the MTEP signal at around 200 K is almost same in magnitude and about five times less than AMR at 4.2 K which suggests MTEP is of the same order or even be larger than AMR.

The effect of magnetization on MTEP is also studied using a sample consist of a bilayer ferromagnet of CuNi(50)/Py(25) deposited on a sapphire substrate. $Cu_{41}Ni_{59}$ is a weak ferromagnet with a T_c of about 150 K. Figure 6.4a shows the data at $\bar{T} = 185$ K and $\Delta T = 30$ K, where two central sharp peaks appear. These peaks correspond to the Py because of lower coercive field and sharp switching. The data recorded at $\bar{T} = 125$ K, which is lower than the T_c of CuNi, shows two more rather wide peaks besides the main central peaks of Py (see Fig. 6.4b). These additional peaks appearing around 7 mT correspond to the coercive field of CuNi. It demonstrate a strong relation of this effect to magnetization and purely a magnetic domain effect like AMR.

6.4.2 CrO_2

Figure 6.5a shows the temperature dependent TEP for CrO_2 thin films deposited on sapphire and TiO_2 substrates. A room temperature value of -9 μV/K is measured for a CrO_2 film deposited on a sapphire substrate. It decreases linearly with temperature and approaches zero at 100 K. The CrO_2 film deposited on TiO_2 has nonlinear behavior along both the in-plane *c*-axis and the *b*-axis. TEP along the *c*-axis changes sign at 265 K and has a room temperature value of -3 μV/K. CrO_2 has a negative TEP along the *b*-axis with room temperature value of -23 μV/K, which is quite similar to the literature value of -25 μV/K [84], where the crystallographic axis is not mentioned.

Figure 6.5c presents MTEP for a 100 nm thick CrO_2 thin film deposited on a sapphire substrate at $\bar{T} = 178$ k and $\Delta T = 45$ K and in parallel configuration. TEP is maximum in the domain state and starts to decrease with the increase in field. Two strong peaks at 10 mT appear. They correspond to the coercive

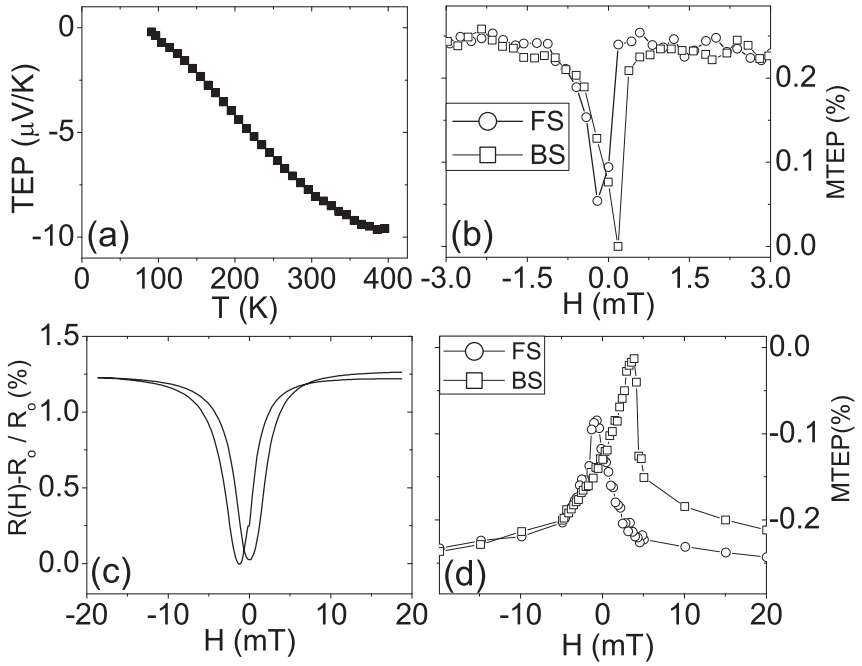

Figure 6.3: (a) Thermoelectric power (TEP) as a function of temperature for a 25 nm thick Py thin film in the temperature range of 100 - 400 K measured with a constant ΔT of 45 K. (b) Magnetic TEP (MTEP) for the same film at $\bar{T}$ = 178 K and ΔT = 45 K, with the field applied along the temperature gradient. (c) Anisotropic Mgnetoresistance (AMR) for the same Py film, measured at 4.2 K. (d) MTEP measurements for a 50 nm thick Co thin film measured at $\bar{T}$ = 178 K with ΔT = 45 K and the field applied along the temperature gradient. Note the difference in sign compared to the data on Py.

field peaks of AMR as shown in the Fig. 6.5d. Behavior of MTEP at higher field is similar to the linear magnetoresistance (MR) in CrO_2 thin films, discussed in detail in Chapter 4. The relative change between maximum and minimum TEP at 200 K is about -3%, which is 15 times larger than AMR signal that even recorded at 4.2 K.

Figure 6.6 shows the data of MTEP and AMR data along both in-plane axes (the *c*-axis and the *b*-axis) for a 100 nm thick CrO_2 thin film deposited on a TiO_2 substrate. For MTEP the field and ΔT are parallel to each other as are field and current (100 μA) for (AMR). Along the *c*-axis the MTEP data show two peaks at the coercive field. CrO_2 has negative relative change in TEP

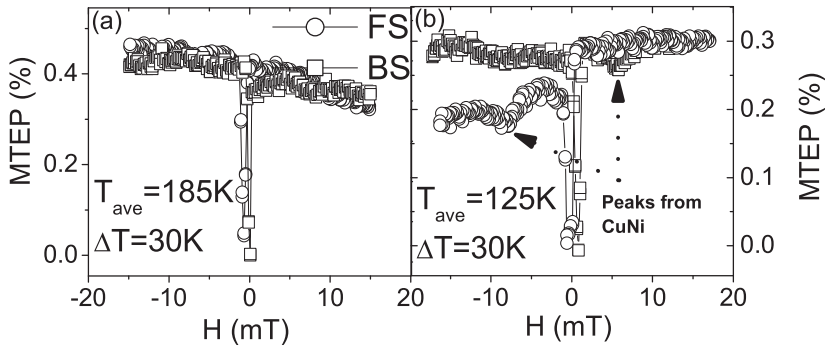

Figure 6.4: MTEP for a multilayer CuNi(50)/Py(25) film deposited on a sapphire substrate. (a) At $\bar{T} = 185$ K, which is higher than Curie temperature of CuNi (150 K), when there are only two strong peaks corresponding coercive filed of Py. (b) At lower temperature $\bar{T} = 125$ K, other two peaks appeared corresponding to CuNi.

with field so in the domain state the TEP is higher than in the saturation state. There are two important notable points in the data presented in the Fig. 6.6. The first point is that MTEP and AMR behave completely similar. In the film the c-axis is the easy magnetic axis, and $H||c$ shows sharp peaks at H_c. Similarly, $H||b$ shows a peak-dip structure both for AMR and for MTEP. The first point is that peaks at coercive field especially along the b-axis there are two peaks just like AMR effect. Second, along the c-axis MTEP increases linearly with the field in the same fashion as in the MR and along the b-axis MTEP is increasing quadratically with the field like MR. These observations show a very close correlation with MTEP and AMR or MR in ferromagnetic materials.

The relative change in MTEP along the c-axis is already 1% just in 50 mT at around 200 K. MTEP to higher fields shows more than 20% relative change, which is a huge signal, 200 times larger than MR at 4.2 K, see Fig. 6.7. Along the b-axis, the relative change in MTEP is 5 times larger than the MR in the range of 0.5 T. MTEP is always much larger than MR regardless of the substrate used to grow the thin films of CrO_2. Here, the saturation of MTEP is also obvious.

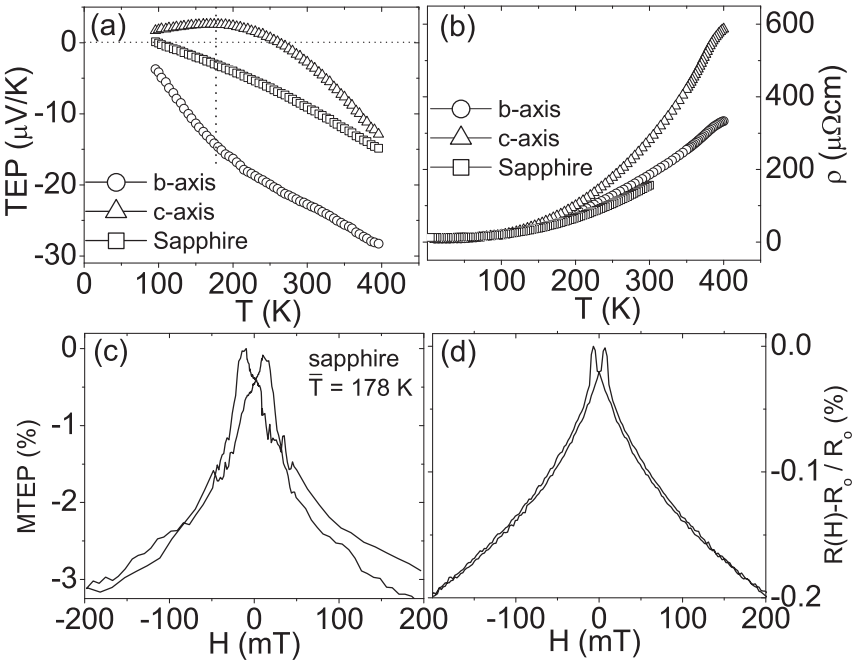

Figure 6.5: (a) Temperature dependent TEP measured in the temperature range of 100 - 400 K on 100 nm thick CrO_2 thin films deposited on sapphire (□) and TiO_2 substrate along the crystallographic *c*-axis (△) and the *b*-axis (◯). TEP changes the sign at 265 K along the *c*-axis. (b) $\rho(T)$ for both films deposited on sapphire and TiO_2 substrates (as also give in Chapter 4). (c) TEP as a function of externally applied field in parallel configuration for CrO_2 film deposited on sapphire at $\bar{T} = 178$ K and $\Delta T = 45$ K. (d) MR probed on same film at 4.2 K in parallel configuration (H || I).

6.5 Discussion

Two aspects of the data can be discussed, the variation of TEP in CrO_2 and Py, and the field dependence found in CrO_2, Py and Co. TEP for normal metals can have electronic contribution as discussed above, but also co-called phonon drag and magnon drag can play a role. In phonon (magnon) drag the phonon (magnon) system is pushed out of equilibrium by scattering with electrons. The resulting net phonon (magnon) momentum yields a drift which also transports heat. At low temperatures (below the Debye temperature) phonon drag has a characteristic T^3 dependence, and a peak at very low

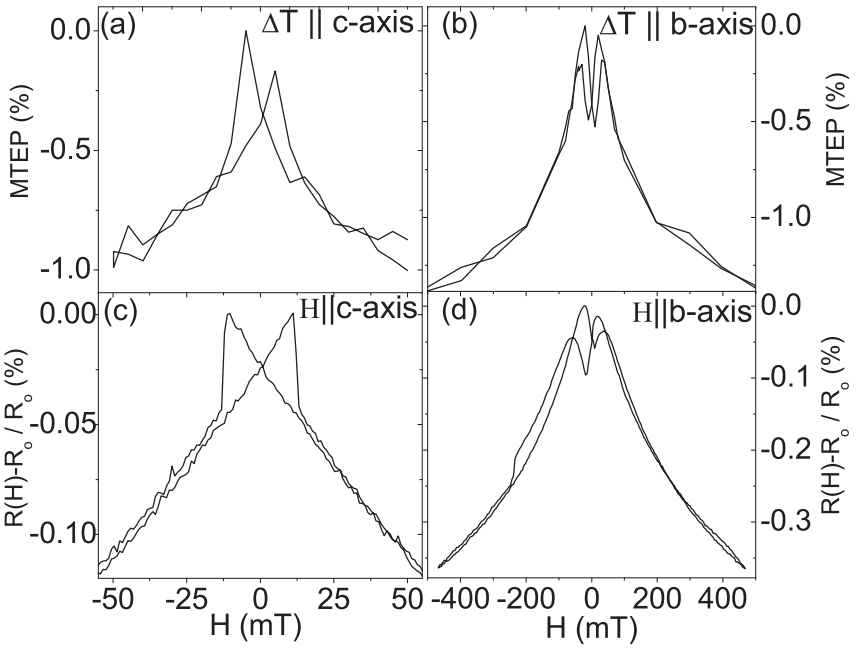

Figure 6.6: (a) MTEP measured at $\bar{T} = 178$ K and $\Delta T = 45$ K, along c-axis of a 100 nm thick CrO_2 thin film deposited on TiO_2 substrate. (b) MTEP along b-axis. (c) AMR measurements with a dc current of 100 μA on same film along c-axis and (d) along b-axis. The peaks corresponding the coercive field are identical for both cases AMR and MTEP.

temperarures. Magnon drag has a $T^{3/2}$ dependence which makes it difficult to distinguish between phonon and diffusive contributions. The TEP measured in Py (Fig. 6.3a) shows more or less linear behavior between 300 K and 100 K indicating that the electronic contribution dominates. In CrO_2, films deposited on sapphire show a linear relation like Py. The films on TiO_2 show somewhat more variations, as well as a difference between the c-axis and the b-axis. What is remarkable is the change in behavior around 200 K. Along the b-axis there is a kink visible followed by a fast decrease of the TEP. Along the c-axis the TEP is already close to zero but flattens fully below 200 K. We compare this behavior with that of the carrier concentration $n(T)$ found in Chapter 4 see Fig. 6.8. It seems probable that the TEP changes its slope below 200 K is linked with the decrease in $n(T)$, which is obvious along the b-axis.

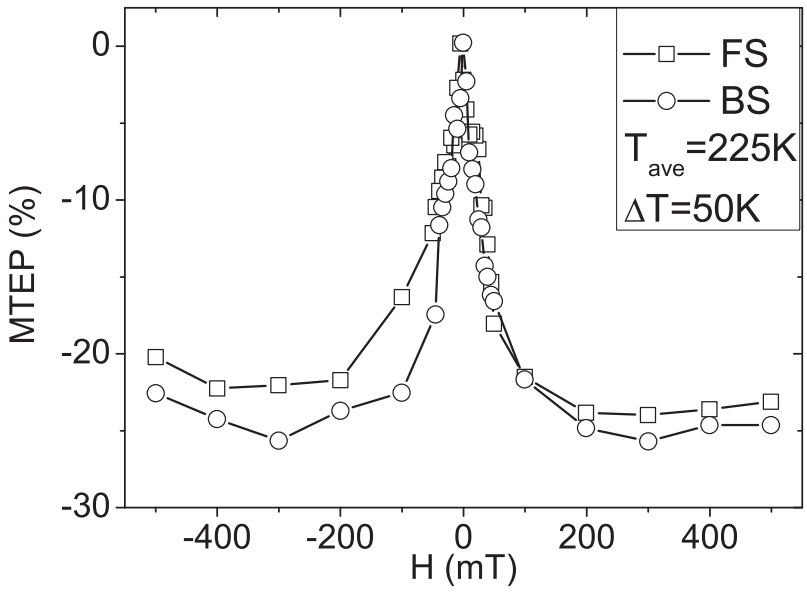

Figure 6.7: MTEP measurements along the c-axis of a 100 nm thick CrO_2 film deposited on a TiO_2 substrate at $\bar{T} = 225$ K and $\Delta T = 50$ K with hot point at 250 K. Maximum relative change in MTEP is of the order of 20%.

Next we turn to the variation of TEP with magnetic field. For Py (Fig. 6.3b-c) it is clear that MTEP and AMR show very similar behavior. In the domain state the AMR shows a lower resistance (field || current), which MTEP shows a lower voltage (field || thermal gradient). Note that the AMR was measured at 4.2 K, the effect at 200 K is much smaller. MTEP for Co shows similar MTEP behavior, except that the thermal voltage now increases in the domain state when compared to the saturated state. This is a puzzling result. It makes clear that electron scattering by magnetic domain walls is the primary mechanism for both AMR and MTEP, but the sign change is not easy to explain although not measured here, it is well known that the AMR has the same sign for Co and Py, which therefore also might have been expected for MTEP.

For CrO_2 it is clear that the MTEP behavior is very much linked to MR, both in the low-field and in the high-field regime. Looking at Fig. 6.6, the MTEP behavior faithfully mimics the MR, both for the situations H $||c$ (easy axis) and H $||b$ interesting to note is that the MTEP variation is large, of the order of 1%, which is both significantly larger than the MTEP effect in Py,

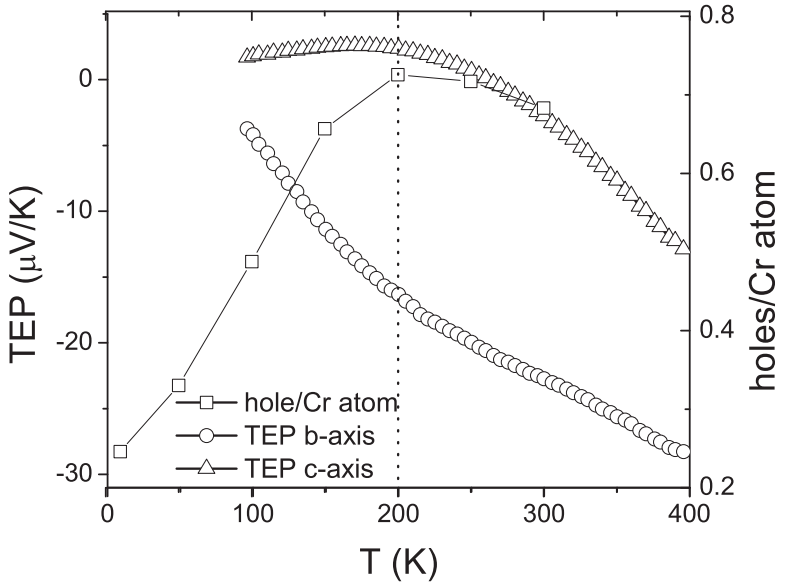

Figure 6.8: Temperature dependent TEP and carrier concentration of a 100 nm thick CrO_2 film deposited on a TiO_2 substrate. An obvious change in the slope of the TEP occurs around 200 K where the carrier concentration starts to decrease.

and than the AMR effects in general. The variations of MTEP is such that the thermopower increased in the domain state. This should follow from the relaxation rate term $\frac{\tau_\epsilon'}{\tau_\epsilon}$ in Eq. 6.16, but this is not yet completely understood.

The high field variations are also similar, and again it is noticed that the MTEP variations are very large. For the sapphire-based film the MTEP change at $\bar{T} = 178$ K is 3% between 0 mT and 200 mT, for the TiO_2-based film ($\Delta T||c$) is 1% up to 50 mT at the same temperature. An even much larger effect for $\Delta T||c$ is measured at $\bar{T} = 225$ K, 25% in a field of 200 mT. There is not yet much to connect to in the experimental or therotical literature. The comparison of Py and CrO_2 indicated that the high spin polarization of the CrO_2 is connected to the strong influence of the magnetic scattering on the heat transport. In high field the electronic structure must play a role. The c-axis TEP shows a sign change around 250 K, and the large variation of the MTEP close to this temperature is possibly connected to this sign change.

More measurements are needed to clarify this behavior.

6.6 Conclusions

The Anisotropic magnetothermoelectric power was investigated in various ferromagnetic thin films, of $Ni_{80}Fe_{20}$ (Permalloy; Py), Co and CrO_2 at temperatures in the range of 100 K to 400 K. The temperature dependent TEP of a Py film is linear like a CrO_2 film deposited on sapphire. For CrO_2 film deposited on TiO_2 is nonlinear with a sign change at 265 K along the *c*-axis and such variation of the TEP with temperature we signal a possible link with the decrease of the carrier concentrations. The main conclusion is that the MTEP behavior is closely linked to the MR. Partially spin polarized thin films of Py and Co show as opposite sign, which is somewhat surprising. The CrO_2 films, deposited both on sapphire and on TiO_2, show large relative changes of the MTEP. In the AMR regime that values are of the order of 1%, at least an order of magnitude larger than the AMR. Along the *c*-axis, the MTEP variation even reaches 25% at a temperature close to a sign change of the TEP.